Available online at www.sciencedirect.com

ScienceDirect

journal homepage: www.elsevier.com/locate/ajps

Original Research Paper

Non-isothermal dehydration kinetic study of aspartame hemihydrate using DSC, TGA and DSC-FTIR microspectroscopy

Wei-hsien Hsieh [*,1], *Wen-ting Cheng*, *Ling-chun Chen*, *Shan-yang Lin* [*,1]

Department of Biotechnology and Pharmaceutical Technology, Yuanpei University of Medical Technology, Hsin Chu 30015, Taiwan, China

ARTICLE INFO

Article history:
Received 29 September 2017
Received in revised form 5 November 2017
Accepted 4 December 2017
Available online 8 December 2017

Keywords:
Aspartame (APM) hemihydrate
DSC/TGA
DSC-FTIR
Dehydration
Activation energy
DKP formation

ABSTRACT

Three thermal analytical techniques such as differential scanning calorimetry (DSC), thermal gravimetric analysis (TGA) using five heating rates, and DSC-Fourier Transform Infrared (DSC-FTIR) microspectroscopy using one heating rate, were used to determine the thermal characteristics and the dehydration process of aspartame (APM) hemihydrate in the solid state. The intramolecular cyclization process of APM anhydrate was also examined. One exothermic and four endothermic peaks were observed in the DSC thermogram of APM hemihydrate, in which the exothermic peak was due to the crystallization of some amorphous APM caused by dehydration process from hemihydrate to anhydride. While four endothermic peaks were corresponded to the evaporation of absorbed water, the dehydration of hemihydrate, the diketopiperazines (DKP) formation via intramolecular cyclization, and the melting of DKP, respectively. The weight loss measured in TGA curve of APM hemihydrate was associated with these endothermic peaks in the DSC thermogram. According to the Flynn–Wall–Ozawa (FWO) model, the activation energy of dehydration process within 100–150 °C was about 218 ± 11 kJ/mol determined by TGA technique. Both the dehydration and DKP formation processes for solid-state APM hemihydrate were markedly evidenced from the thermal-responsive changes in several specific FTIR bands by a single-step DSC-FTIR microspectroscopy.

1. Introduction

A challenge for establishing the most thermodynamically stable polymorph of an active pharmaceutical ingredient (API) in the oral marketed formulations has been rising continuously in the recent years, since different pharmaceutical polymorphs may alter its physicochemical properties and result in various pharmaceutical, therapeutic, legal and/or commercial problems [1–4]. In fact, an API in each solid dosage form ideally receives

* *Corresponding authors*. Department of Biotechnology and Pharmaceutical Technology, Yuanpei University of Medical Technology, Hsin Chu 30015, Taiwan, China. Tel.: +886 03 6102439.
E-mail addresses: weihsien@mail.ypu.edu.tw (W. Hsieh), sylin@mail.ypu.edu.tw (S. Lin).
Peer review under responsibility of Shenyang Pharmaceutical University.
[1] These authors contributed equally.
https://doi.org/10.1016/j.ajps.2017.12.001

regulatory approval for only a single crystal form or polymorph and avoids any polymorphic transition in the formulation during the manufacturing process and storage [5,6]. According to the FDA's ANDAs guidance, polymorphic forms refer to crystalline, amorphous forms, solvate and hydrate forms [7]. More than one-third of drugs used in the pharmaceutical industry possess various polymorphs, and approximately at least one-third of which have been reported to have hydrate form in various pharmacopeias [8,9].

Generally, pharmaceutical hydrates exhibit a wide range of physical and chemical properties, solubility, stability, and bioavailability [10–12]. The hydrate formation/dehydration may occur during various pharmaceutical unit operations or during normal storage of the finished product, in which the phase transition is frequently encountered [13,14]. Since the dehydration-induced phase transition is accompanied by a change in the physicochemical properties, different dehydration conditions can have an effect on the behavior of the final product [15]. When the hydrates are dehydrated, the type of hydrate and the processing condition used will result in a certain type of dehydrated hydrate whose properties can be slightly different from the pure anhydrate [15,16]. Classic dehydration kinetics is treated as a solid-state reaction, many solid-state kinetic studies on desolvation reactions or polymorphic transformations have gained much interest in the preformulation and formulation design [14,17–19]. Due to the dehydration process that may cause a structural change and consequently change the solubility, stability, and bioavailability of the APIs [2,20–23], it is necessary to understand the hydration or dehydration behavior of a hydrated drug substance in the development of a stable drug formulation.

Aspartame (l-aspartyl-l-phenylalanine methyl ester, APM) is a dipeptide sweetener extensively used in the food, beverage, and pharmaceutical industries [24,25]. APM was reported to have a variety of solvatomorphic forms, that are one anhydrous form, two hemihydrate forms (Forms I and II) and a dihemihydrate [26–28]. Now, the commercially available APM is hemihydrate corresponding to Form II. As an approved excipient, APM has been successfully applied in many compressed solid dosage forms from 1.1 mg to 65 mg per unit [25]. However, APM in the solid state may easily form a diketopiperazine derivative (DKP) via intramolecular cyclization reaction, which is a key degradation product of APM during long-term storage [29–31]. Numerous investigations have focused on the isothermal and non-isothermal analyses of solid-state stability of APM [29,30,32–34]. However, there were less studies directed on the kinetics and/or energy changes in the dehydration process of APM hemihydrate [26,28].

Thermal analysis is a well-known technique for characterization of APIs in terms of structural and stability investigations [34–36], differential scanning calorimetry (DSC) and thermal gravimetric analysis (TGA) are respectively used to measure the changes in enthalpy or weight of different APIs or excipients as a function of temperature over time [34–36]. In addition, a powerful analytical technique by combining a DSC with the Fourier Transform Infrared (DSC-FTIR) microspectroscopy can give simultaneously thermodynamic and spectroscopic information of a sample and may serve as an accelerated stability test in preformulation study [31,37,38]. Several compounds such as linsinopril dihydrate, trehalose dihydrate, raffinose pentahydrate and metoclopramide HCl monohydrate had been investigated by above three thermal analyses in our previous studies [39–42]. In the present studies, the thermal characteristics and stability, and dehydration kinetics of APM hemihydrate were investigated by the above three thermal analytical techniques. Particularly, the activation energy of the dehydration process of APM hemihydrate was also non-isothermally estimated by TGA technique. In addition, by smearing a small amount of sample on one piece of KBr disk prepared for DSC-FTIR microspectroscopic study was also attempted.

2. Materials and methods

2.1. Materials

Aspartame (APM) hemihydrate ($C_{14}H_{18}O_5N_2 \cdot 0.5H_2O$) was purchased from Tokyo Kasei Indus. Co. Ltd. (Tokyo, Japan) and was used without further treatment. KBr crystals for disk preparation were purchased from JASCO Spectroscopic Co. Ltd. (Tokyo, Japan).

2.2. Differential scanning calorimetry (DSC)

Approximately 5–7 mg of each APM sample was placed inside the DSC pan for thermal analysis. All the DSC thermograms of APM samples were respectively determined by using differential scanning calorimetry (DSC Q20, TA Instruments, Inc., New Castle, DE, USA) from 30 to 285 °C at different heating rates with an open pan system under nitrogen purge at 30–40 ml/min. These non-isothermal studies were performed at the following heating rates: 1, 3, 5, 10 and 15 °C/min. The instrument was calibrated for temperature and heat flow using a high-purity indium as a standard.

2.3. Thermogravimetric analysis (TGA)

Thermogravimetric analysis (TGA Q50, TA Instruments, Inc., New Castle, DE, USA) was also used to determine the weight loss in the open system with a nitrogen purge at 30–40 ml/min. A quantity of 5–7 mg of APM sample was used for each test. Non-isothermal experimental runs were performed at five different heating rates of 1, 3, 5, 10 and 15 °C/min. Prior to the experimental runs, the instrument was calibrated for precise temperature and weight readings.

2.4. Karl Fischer titration

The water content of the solid forms of APM hemihydrate was determined by Karl Fischer moisture titrator (MKC-520, Kyoto Electronics Manufacturing Co. Ltd., Tokyo, Japan). Samples (5–7 mg) were accurately weighed and quickly transferred to the titration vessel containing dehydrated methanol prior to titration, stirring for 1 minute and titrating to the end-point with Karl Fischer reagent.

2.5. DSC-FTIR microspectroscopic study

A small amount of APM hemihydrate powder was previously smeared on one piece of KBr disk prepared and then carefully

pressed by an IR spectrophotometric hydraulic press (Riken Seiki Co., Tokyo, Japan) under 400 kg/cm^2 for 15 s. This compressed KBr disk was then placed directly onto a micro hot stage (DSC microscopy cell, FP 84, Mettler, Greifensee, Switzerland) and directly determined by FTIR microspectroscopy (IRT-5000-16/FTIR-6200, Jasco Co., Tokyo, Japan) with a mercury cadmium telluride (MCT) detector. The operation was performed in the transmission mode. FTIR spectra were generated by co-addition of 256 interferograms collected at 4 cm^{-1} resolution. The temperature of the DSC microscopy cell was monitored with a central processor (FP 80HT, Mettler, Switzerland). The heating rate of the DSC assembly was controlled at 3 °C/min under ambient conditions. The compressed KBr disk was previously equilibrated to the starting temperature (30 °C) and then heated from 30 to 300 °C. At the same time, the thermal-responsive IR spectra were recorded when the sample disk was heated on the DSC micro hot stage.

3. Results and discussion

3.1. *Identification of APM sample determined by DSC and TGA techniques*

Fig. 1 shows the DSC thermogram and TGA curve of APM sample determined by using a heating rate of 1 °C/min. It clearly indicates that four endothermic peaks at 47, 111, 173 and 232 °C, and one exothermic peak at 122 °C were observed in the A~D regions of DSC thermogram for APM sample. The former two DSC endothermic peaks at 47 and 111 °C in the A~B regions were due to the evaporation of absorbed water and dehydration of hemihydrate, which were confirmed by the total weight loss of 3.23% (w/w) in TGA curve before 150 °C. The weight loss of 1.89% (w/w) that occurred in the temperature range of 100–150 °C was corresponded to the exact dehydration from APM hemihydrate to APM anhydrate, whereas the initial weight loss at approximately 1.34% (w/w) between 30 and 100 °C was due to the evaporation of adsorbed water and partial dehydration from APM hemihydrate. Here, the total weight loss of water below 150 °C is 3.23% (w/w), was close to the Karl Fischer titration value of 3.76% (w/w) for APM hemihydrate. Since the theoretical water content of pure APM hemihydrate (excluding absorbed water) is 2.97% (w/w), this indicates that about 0.26% (w/w) absorbed water on the surface of APM hemihydrate was determined by TGA method. This demonstrates that the APM sample used in the present study was hemihydrate form, which was consistent with the commercially available APM hemihydrate (Form II) used in other studies [26,27].

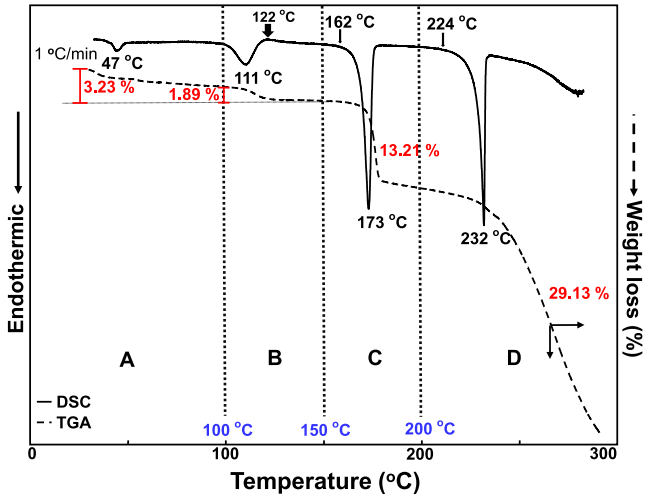

Fig. 1 – DSC thermogram and TGA curve of APM sample determined using a heating rate of 1 °C/min.

Another two endothermic peaks at 173 and 232 °C in the C~D regions corresponded to the DKP formation due to intramolecular cyclization in the APM anhydrate and the melting point of DKP, respectively. Obviously, the corresponding TGA curve illustrates that the 13.21% (w/w) of weight loss within 150–200 °C was attributed to the loss of methanol molecule with the formation of DKP from the APM anhydrate via intramolecular cyclization [26,27,32,33]. This is consistent with the results of Leung and Grant that APM anhydrate underwent a cyclization reaction which involved an intramolecular aminolysis with release of methanol to form the cyclic compound DKP [29], However, this value of 13.21% (w/w) somewhat deviated from the theoretical weight loss of methanol (10.55% (w/w)). This might possibly be because a small amount of residual water was held either by strong ion-dipole interactions between zwitterionic aspartame and dipolar water molecules or by occlusion onto the hydrophobic surface of the tiny crystallites in the inner columnar structure of the crystals [26,43].

The weight loss of 29.13% (w/w) beyond 200 °C was mainly attributed to the degradation of DKP. On the other hand, an exothermic peak at 122 °C was also observed, which was corresponded to the crystallization of some amorphous APM produced by dehydration process of the hemihydrate [44]. The formation of some amorphous content in the APM mixture within the temperature range of 100–150 °C had been confirmed by variable temperature X-ray powder diffractometry [44]. This exothermic peak in the DSC thermogram was also observed in the DSC results of Leung et al. [26].

3.2. *Non-isothermal dehydration study by TGA technique*

It is well-known that the Flynn–Wall–Ozawa (FWO) method is one of the model-free methods to study the solid-state kinetic parameters in solid-state interactions via isoconversional calculation for non-isothermal studies [45–47]. The FWO method involves measuring the temperatures corresponding to fixed values of conversion (α) from experiments at different heating rates through an isoconversional approach based on the Doyle approximation [48,49]. This is one of the integral approaches used to calculate the apparent activation energy (*Ea*) without prefixing the reaction order as given by:

$$\log\beta = \log[ZEa/f(\alpha)R] - 0.457\,(Ea/RT) - 2.315$$

where, β, heating rate; Z, pre-exponential factor; *Ea*, activation energy (J/mol); R, gas constant; *f*(α), the integral conversion function; T, temperature (K) at constant conversion.

For a constant conversion, a plot of natural logarithm of heating rates, log β, versus 1/T obtained from thermal curves

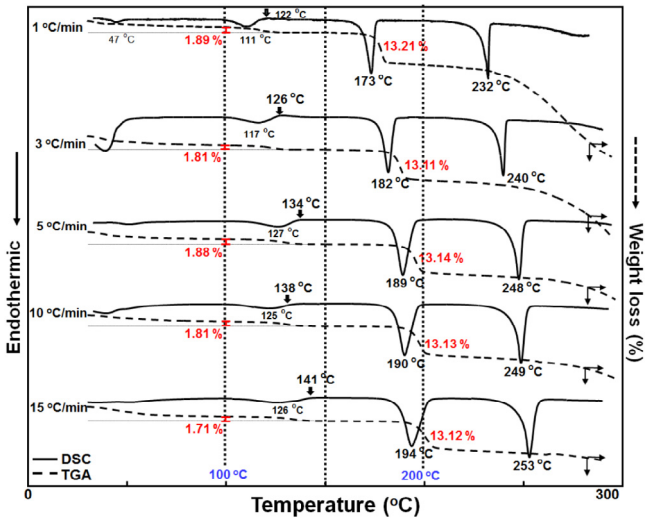

Fig. 2 – DSC thermograms and TGA curves of APM hemihydrate determined by different heating rates.

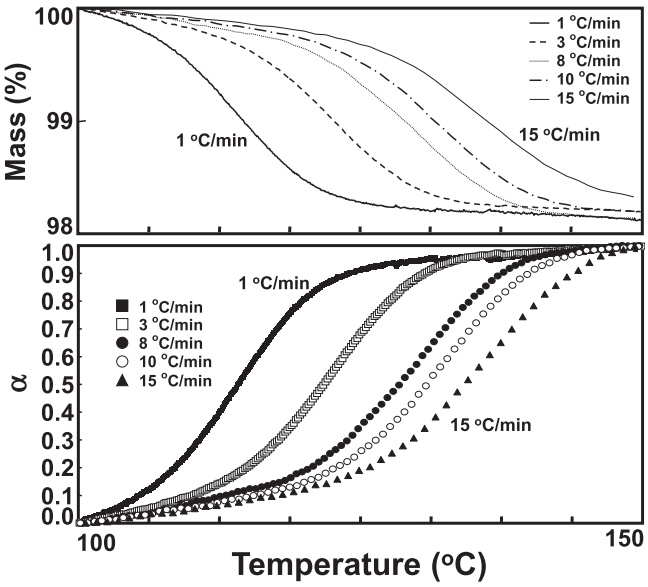

Fig. 3 – Typical TGA curves (upper) and α-T plots (lower) for the thermal dehydration of APM hemihydrate at different heating rates.

recorded at different heating rates will be a straight line whose slope (–0.457 (*Ea*/R)) allows evaluation of the activation energy.

In this study, the non-isothermal dehydration studies based on the FWO method were performed at the following heating rates: 1, 3, 5, 10, and 15 °C/min by using DSC and TGA determinations. Fig. 2 displays the DSC thermograms and TGA curves of APM hemihydrate determined by five heating rates of 1, 3, 5, 10, and 15 °C/min. Clearly, the effect of different heating rates on the shifting of peak temperatures in the DSC thermograms was distinctly shown. By increasing the heating rates, all the peak positions either exothermic or endothermic peaks shifted toward the higher temperatures because it had less time at any specific temperature [50,51]. In the TGA curves, however, the weight loss was about 1.71%–1.89% (w/w) within 100~150 °C due to dehydration and was about 13.11%–13.21% (w/w) within 150–200 °C attributed to intramolecular cyclization, respectively. They are almost constant in each temperature range. The TGA data will be used for the determination of the activation energy using the FWO method.

These different profiles for mass loss and conversion levels (α) of APM hemihydrate at different heating rates are shown in Fig. 3. Similar mass loss profiles were observed. The temperature ranges were shifted to higher temperatures as the heating rate increased. In addition, linear plots of log β versus 1/T corresponding to nine conversion levels (α = 10%–90%) by the FWO method are also obtained (Fig. 4A). All the plots have a strong negative linear relationship ($r^2 > 0.99$) except 10% conversion line. The apparent activation energies (*Ea*) were calculated from the slope of a linear regression line for a particular *α*. The variation in apparent *Ea* calculated with various conversion levels is shown in Fig. 4B. Obviously, the *Ea* decreased as the reaction progresses at low conversion, which was related to the characteristics of reversible thermal decomposition processes like dehydration [52]. Except 10% conversion, all the *Ea* data for the dehydration process of APM hemihydrate were similar and calculated to be 218 ± 11 kJ/mol. This value was well close to that of the 214 kJ/mol reported by Rastogi et al. using variable temperature X-ray powder diffractometry [44], indicating the reliability of this TGA technique for evaluation of dehydration kinetics of APM hemihydrate.

3.3. *Non-isothermal DSC-FTIR microspectroscopic study*

Recently, a powerful analytical technique by combining a thermal analyzer with the FTIR (DSC-FTIR) microspectroscopy has been widely used in various fields for giving simultaneous thermodynamic and spectroscopic identification of different materials [31,37,38,53,54]. In our laboratory, this unique simultaneous DSC-FTIR microspectroscopy has been considerably applied to rapidly examine the thermal-induced characterization of intramolecular cyclization of diketopiperazine or anhydride formation, lactamization or decarboxylation, and polymorphic interconversion and co-crystal formation of polymers or drugs in the solid state [31–33,37,38,54–57].

In the present study, only a very small amount of APM sample was used and smeared on one piece of KBr disk prepared and then carefully pressed by an IR spectrophotometric hydraulic press. This method was different from that of our previous studies by sealing and pressing APM sample within two pieces of KBr disks [32,33]. Obviously, the FTIR peak intensities of APM hemihydrate made by pressing it on one piece of KBr disk are sharper than that of the sample sealed within two pieces of KBr disks. The FTIR spectral changes of APM hemihydrate prepared from one piece of KBr disk were more clearly observed, as compared with our previous reports [32,33].

Thermal-dependent three-dimensional FTIR plots of APM hemihydrate in the heating process are displayed in Fig. 5. Before heating (at 30 °C), several characteristic FTIR absorption bands at 3310 cm^{-1} (hydrogen-bonded N—H stretch), 3066–2951 cm^{-1} (aromatic and aliphatic C—H stretch), 1738 and 1662 cm^{-1} (CC═CO stretch of ester and amide I), 1587 cm^{-1} (*asy*COO^- stretch), 1551 cm^{-1} (N—H bend of amide II), 1496 cm^{-1}

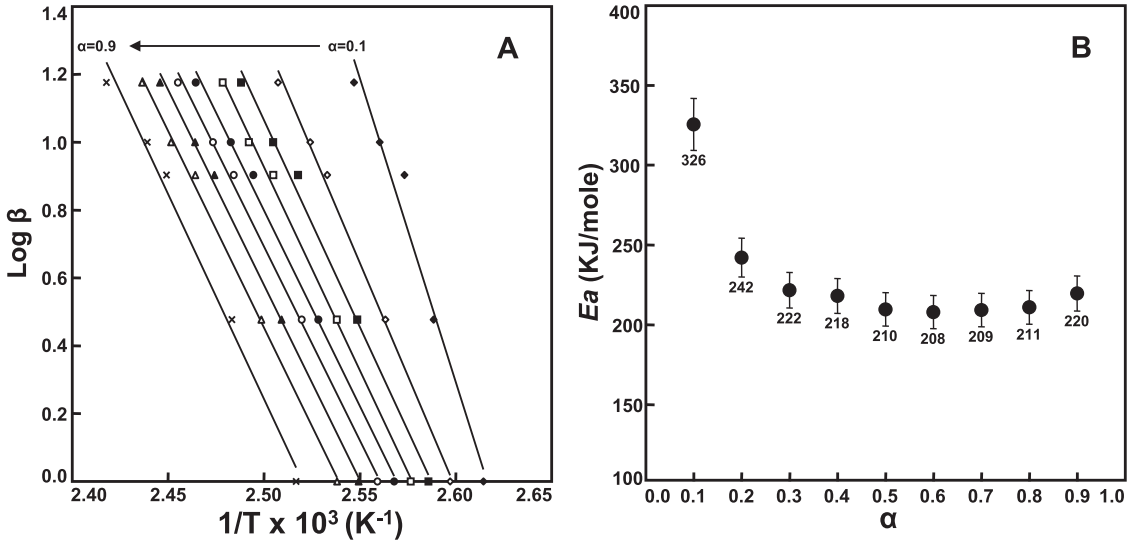

Fig. 4 – The FWO plots (A) and the plot of *Ea* versus α (B) for the thermal dehydration of APM hemihydrate at different heating rates.

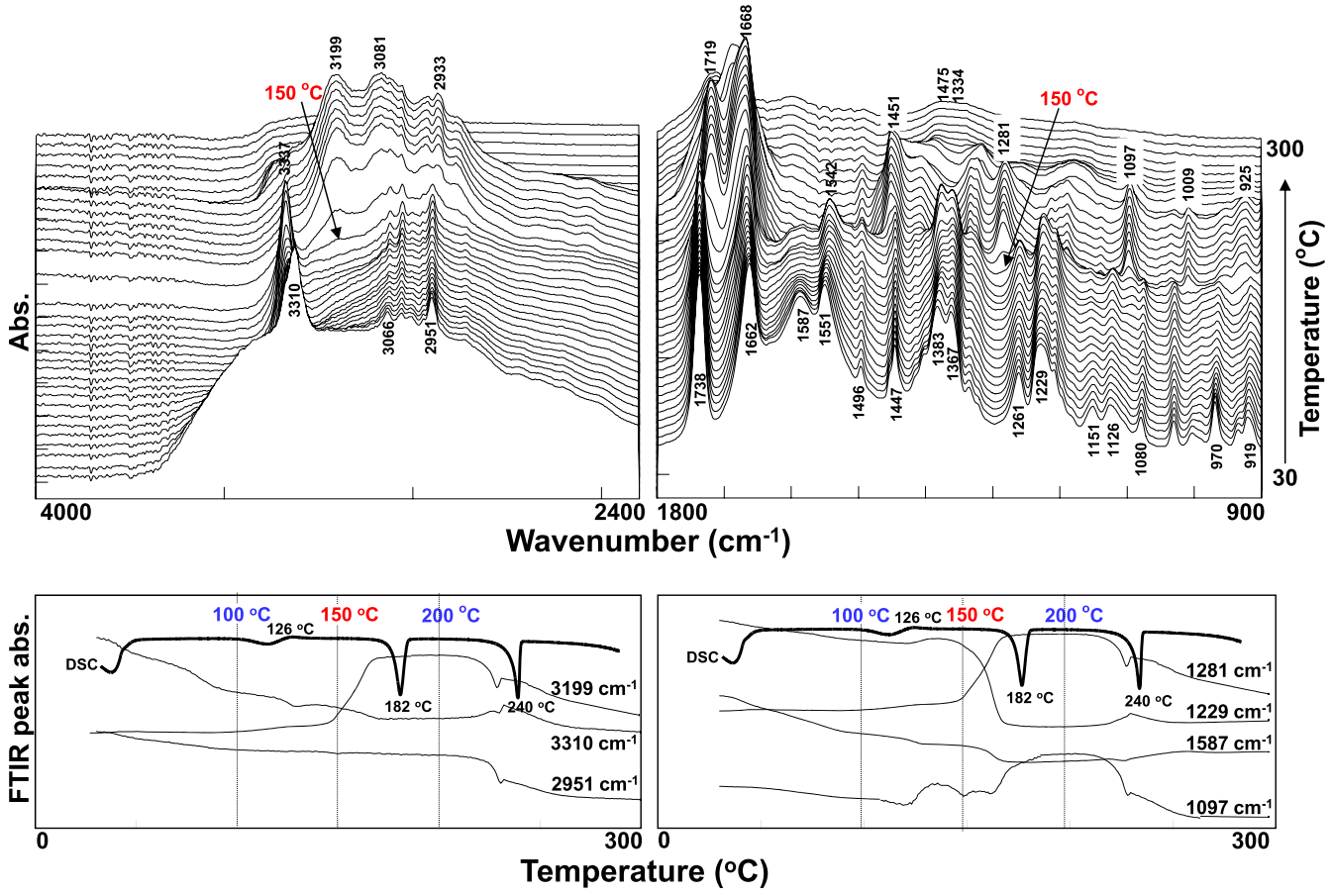

Fig. 5 – Thermal-dependent changes in three-dimensional FTIR plots of APM hemihydrate and its changes in FTIR peak intensity of several specific peaks.

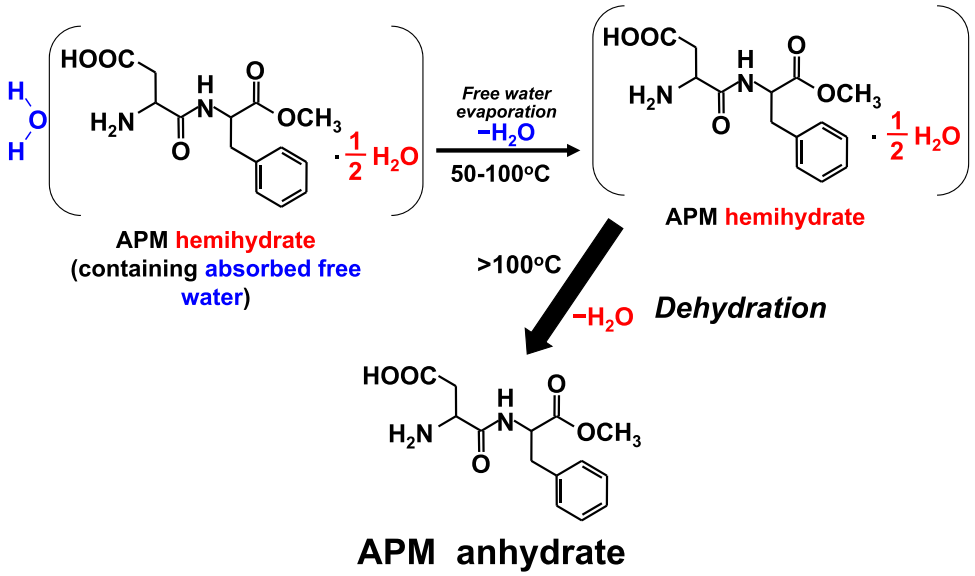

Fig. 6 – The continuous pathway for the absorbed water evaporation and dehydration process of APM hemihydrate.

(C═C stretch of aromatic benzene ring), 1447 cm^{-1} (aromatic C—C stretch), 1383 cm^{-1} (C—H bend), 1367 cm^{-1} (syCOO^- stretch), 1261 cm^{-1} (methoxyl group), and 1229 cm^{-1} (C—O stretch of ester) were observed in the FTIR spectrum of APM hemihydrate [26,27,58].

As the temperature of the sample was increased, all the FTIR spectral positions and peak intensities were maintained for a period of time and then altered. Some positions and intensities of FTIR peaks were gradually changed with temperature. The thermal-dependent changes in three-dimensional FTIR plots of APM hemihydrate are clearly displayed in Fig. 5. Before 150 °C, several unique IR peaks at 3310, 1587, 1551 1383, 1367, 1261 and 1229 cm^{-1} were gradually shifted and disappeared with the increase of temperature. This was attributed to the thermal-induced reduction of the hydrogen bonding among water, NH^+_3 and COO^- of APM hemihydrate within 50~100 °C ranges and the thermal-induced dehydration from APM hemihydrate to APM anhydrate in a temperature range between 100 and 150 °C (Fig. 6). The appearance of 3337 cm^{-1} (free N—H stretch) shifted from 3310 cm^{-1} (hydrogen-bonded N—H stretch) was corresponded to the thermal-induced evaporation of free absorbed water and dehydration of APM hemihydrate (Fig. 5).

When the temperature was beyond 150 °C, however, the three-dimensional FTIR plots were significantly changed. In particular, the IR peak at 3337 cm^{-1} assigned to the asymmetric stretching vibration of free NH_2 disappeared, but two new peaks at 3199 and 3081 cm^{-1} corresponding to the stretching NH of 3-carboxymethyl-6-benzyl-2,5-diketopiperazine (DKP) appeared [26,27,31–33]. In addition, the peak at 1738 cm^{-1} due to the carbonyl group of ester disappeared gradually but a new peak at 1719 cm^{-1} assigned to the carbonyl CC═CO of carboxylic acid slowly increased. Moreover, the peak at 1662 cm^{-1} corresponding to the amide CC═CO of APM also shifted to the 1668 cm^{-1} of DKP CC═CO with an intensity which was twice stronger due to the two diketones formed in the DKP ring. The amide II-related N—H peak at 1542 cm^{-1} shifted from 1551 cm^{-1} also disappeared, possibly due to the complete formation of DKP. With the liberation of methanol from the APM molecule, the peaks at 1383 (C—H bending), 1261 (methoxyl group) and 1229 cm^{-1} (C—O stretch of ester) disappeared, and the peaks at 1281, 1097, 1009 and 925 cm^{-1} assigned to C—N and lactam ring stretchings of DKP gradually appeared. The changes in FTIR peak absorbance were clearly observed for IR peaks at 3199, 1281, 1229 and 1097 cm^{-1}. Once the temperature was raised over 240 °C, the DKP products began to decompose extensively [29,58]. This suggests that the simultaneous DSC-FTIR combined technique could easily confirm the dehydration and intramolecular cyclization of DKP formation from the solid-state APM hemihydrate in a single-step treatment.

4. Conclusions

The thermal characteristics and the dehydration kinetics of APM hemihydrate and DKP formation of APM anhydrate were successfully studied using DSC, TGA and DSC-FTIR microspectroscopy with non-isothermal techniques. One exothermic and four endothermic peaks were observed in the DSC thermogram of APM hemihydrate. In addition, the activation energy of dehydration process was about 218 ± 11 kJ/mol determined by TGA method. The thermal-dependent structural re-arrangement of the APM molecule was clearly and stepwise observed from the changes in the FTIR spectra using DSC-FTIR determination. Rapid and simultaneous detection of both dehydration and intramolecular cyclization processes for solid-state APM hemihydrate after smearing on one piece of KBr disk were clearly evidenced by DSC-FTIR microspectroscopy.

Conflicts of interest

The authors declare that there are no conflicts of interest.

Acknowledgments

The authors alone are responsible for the content and writing of this article.

REFERENCES

[1] Singhal D, Curatolo W. Drug polymorphism and dosage form design: a practical perspective. Adv Drug Deliv Rev 2004;56(3):335–47.
[2] Censi R, Di Martino P. Polymorph impact on the bioavailability and stability of poorly soluble drugs. Molecules 2015;20(10):18759–76.
[3] Higashi K, Ueda K, Moribe K. Recent progress of structural study of polymorphic pharmaceutical drugs. Adv Drug Deliv Rev 2017;117:71–85.
[4] Bauer JF. Polymorphism: a critical consideration in pharmaceutical development, manufacturing, and stability. J Valid Technol 2008;14(4):15–23.
[5] Grant DJ, Byrn SR. A timely re-examination of drug polymorphism in pharmaceutical development and regulation. Adv Drug Deliv Rev 2004;56(3):237–9.
[6] Byrn S, Pfeiffer R, Ganey M, et al. Pharmaceutical solids: a strategic approach to regulatory considerations. Pharm Res 1998;12(7):945–54.
[7] FDA. ANDAs: Pharmaceutical Solid Polymorphism, "Chemistry, Manufacturing, and Controls Information," July 2007.
[8] Qu H, Munk C, Cornett J, et al. Influence of temperature on solvent-mediated anhydrate-to-hydrate transformation kinetics. Pharm Res 2011;28(2):364–73.
[9] Bajpai A, Scott HS, Pham T, et al. Towards an understanding of the propensity for crystalline hydrate formation by molecular compounds. IUCrJ 2016;3(Pt 6):430–9.
[10] Khankari RK, Grant DJ. Pharmaceutical hydrates. Thermochim Acta 1995;248:61–79.
[11] Giron D, Goldbronn C, Mutz M, et al. Solid state characterizations of pharmaceutical hydrates. J Therm Anal Calorim 2002;68(2):453–65.
[12] Franklin SJ, Younis US, Myrdal PB. Estimating the aqueous solubility of pharmaceutical hydrates. J Pharm Sci 2016;105(6):1914–9.
[13] Koradia V, de Diego HL, Elema MR, et al. Integrated approach to study the dehydration kinetics of nitrofurantoin monohydrate. J Pharm Sci 2010;99(9):3966–76.
[14] Vippagunta SR, Brittain HG, Grant DJ. Crystalline solids. Adv Drug Deliv Rev 2001;48(1):3–26.
[15] Trasi NS, Boerrigter SX, Byrn SR, et al. Investigating the effect of dehydration conditions on the compactability of glucose. Int J Pharm 2011;406(1–2):55–61.
[16] Ono M, Tozuka Y, Oguchi T, et al. Effects of dehydration temperature on water vapor adsorption and dissolution behavior of carbamazepine. Int J Pharm 2002;239(1–2):1–12.
[17] Sheng J, Venkatesh GM, Duddu SP, et al. Dehydration behavior of eprosartan mesylate dihydrate. J Pharm Sci 1999;88(10):1021–9.
[18] Khawam A, Flanagan DR. Basics and applications of solid-state kinetics: a pharmaceutical perspective. J Pharm Sci 2006;95(3):472–98.
[19] Rodríguez-Spong B, Price CP, Jayasankar A, et al. General principles of pharmaceutical solid polymorphism: a supramolecular perspective. Adv Drug Deliv Rev 2004;56(3):241–7.
[20] Carvalho PS, de Melo CC, Ayala AP, et al. Reversible solid-state hydration/dehydration of paroxetine HBr hemihydrate: structural and thermochemical studies. Cryst Growth Des 2016;16(3):1543–9.
[21] Shah SM, Jain AS, Kaushik R, et al. Preclinical formulations: insight, strategies, and practical considerations. AAPS PharmSciTech 2014;15(5):1307–23.
[22] Byrn S, Zografi G, Chen X. Solid-state properties of pharmaceutical materials. 1st ed. USA: John Wiley & Sons, Inc.; 2017.
[23] Bērziņš A, Actiņš A. Dehydration of mildronate dihydrate: a study of structural transformations and kinetics. CrystEngComm 2014;16:3926–34.
[24] Magnuson BA, Carakostas MC, Moore NH, et al. Biological fate of low-calorie sweeteners. Nutr Rev 2016;74(11):670–89.
[25] Niazi SK. Compressed solid products. In: Handbook of pharmaceutical manufacturing formulations, vol. 1. 2nd ed. Boca Raton (FL): CRC Press; 2009. p. 100–1, 210-11.
[26] Leung SS, Padden BE, Munson EJ, et al. Hydration and dehydration behavior of aspartame hemihydrate. J Pharm Sci 1998;87(4):508–13.
[27] Leung SS, Padden BE, Munson EJ, et al. Solid-state characterization of two polymorphs of aspartame hemihydrate. J Pharm Sci 1998;87(4):501–7.
[28] Guguta C, Meekes H, de Gelder R. The hydration/dehydration behavior of aspartame revisited. J Pharm Biomed Anal 2008;46(4):617–24.
[29] Leung SS, Grant DJ. Solid state stability studies of model dipeptides: aspartame and aspartylphenylalanine. J Pharm Sci 1997;86(1):64–71.
[30] Skwierczynski RD. Disorder, molecular mobility, and solid-state kinetics: the two-environment model. J Pharm Sci 1999;88(11):1234–6.
[31] Lin SY, Wang SL. Advances in simultaneous DSC-FTIR microspectroscopy for rapid solid-state chemical stability studies: some dipeptide drugs as examples. Adv Drug Deliv Rev 2012;64(5):461–78.
[32] Lin SY, Cheng YD. Simultaneous formation and detection of the reaction product of solid-state aspartame sweetener by FT-IR/DSC microscopic system. Food Addit Contam 2000;17(10):821–7.
[33] Cheng YD, Lin SY. Isothermal Fourier transform infrared microspectrosopic studies on the stability kinetics of solid-state intramolecular cyclization of aspartame sweetener. J Agric Food Chem 2000;48(3):631–5.
[34] Giron D. Applications of thermal analysis and coupled techniques in pharmaceutical industry. J Therm Anal Calorim 2001;68(2):335–57.
[35] Craig DQM, Reading M. Thermal analysis of pharmaceuticals. 1st ed. Boca Raton (FL): CRC Press; 2006.
[36] Stodghill SP. Thermal analysis – a review of techniques and applications in the pharmaceutical sciences. Am Pharm Rev 2010;13(2):29, 31-6.
[37] Lin SY, Lin CC. One-step real-time food quality analysis by simultaneous DSC-FTIR microspectroscopy. Crit Rev Food Sci Nutr 2016;56(2):292–305.
[38] Lin SY. Simultaneous screening and detection of pharmaceutical co-crystals by the one-step DSC-FTIR microspectroscopic technique. Drug Discov Today 2017;22(4):718–28.
[39] Wang SL, Lin SY, Chen TF. Thermal-dependent dehydration process and intramolecular cyclization of lisinopril dihydrate in the solid state. Chem Pharm Bull 2000;48(12):1890–3.

[40] Lin SY, Chien JL. In vitro simulation of solid-solid dehydration, rehydration and solidification of trehalose dihydrate using thermal and vibrational spectroscopic techniques. Pharm Res 2003;20(12):1926–31.
[41] Cheng WT, Lin SY. Processes of dehydration and rehydration of raffinose pentahydrate investigated by thermal analysis and FT-IR/DSC microscopic system. Carbohydr Polym 2006;64(2):212–7.
[42] Wang SL, Wong YC, Cheng WT, et al. A continuous process for solid-state dehydration, amorphization and recrystallization of metoclopramide HCL monohydrate studied by simultaneous DSC-FTIR microspectroscopy. J Therm Anal Calorim 2011;104(1):261–4.
[43] Hatada M, Jancarik J, Graves B, et al. Crystal structure of aspartame, a peptide sweetener. J Am Chem Soc 1985;107(14):4279–82.
[44] Rastogi S, Zakrzewski M, Suryanarayanan R. Investigation of solid-state reactions using variable temperature X-ray powder diffractometry I. Aspartame hemihydrate. Pharm Res 2001;18(3):267–73.
[45] Vyazovkin S, Dollimore D. Linear and nonlinear procedures in isoconversional computations of the activation energy of nonisothermal reactions in solids. J Chem Inf Comput Sci 1996;36(1):42–5.
[46] Khawam A, Flanagan DR. Solid-state kinetic models: basics and mathematical fundamentals. J Phys Chem B 2006;110(35):17315–28.
[47] Vyazovkin S, Burnham AK, Criado JM, et al. ICTAC kinetics committee recommendations for performing kinetic computations on thermal analysis data. Thermochim Acta 2011;520(1–2):1–19.
[48] Khawam A, Flanagan DR. Role of isoconversional methods in varying activation energies of solid-state kinetics: II. Nonisothermal kinetic studies. Thermochim Acta 2005;436(1–2):101–12.
[49] Pina MF, Zhao M, Pinto JF, et al. An investigation into the dehydration behavior of paroxetine HCl form I using a combination of thermal and diffraction methods: the identification and characterization of a new anhydrous form. Cryst Growth Des 2014;14(8):3774–82.
[50] Tudja P, Khan MZ, Mestrović E, et al. Thermal behaviour of diclofenac sodium: decomposition and melting characteristics. Chem Pharm Bull 2001;49(10):1245–50.
[51] Thomas LC. Use of multiple heating rate DSC and modulated temperature DSC to detect and analyze temperature-time-dependent transitions in materials. Am Lab USA 2001;33:26–9.
[52] Liavitskaya T, Vyazovkin S. Delving into the kinetics of reversible thermal decomposition of solids measured on heating and cooling. J Phys Chem C 2017;121(28):15392–401.
[53] Johnson DJ, Compton DAC, Canale PL. Applications of simultaneous DSC/FTIR analysis. Thermochim Acta 1992;195:5–20.
[54] Lin SY. An overview of advanced hyphenated techniques for simultaneous analysis and characterization of polymeric materials. Crit Rev Solid State Mater Sci 2016;41(6): 482–530.
[55] Lin SY. Molecular perspectives on solid-state phase transformation and chemical reactivity of drugs: metoclopramide as an example. Drug Discov Today 2015;20(2):209–22.
[56] Wang SL, Lin SY, Hsieh TF, et al. Thermal behavior and thermal decarboxylation of 10-hydroxycamptothecin in the solid state. J Pharm Biomed Anal 2007;43(2):457–63.
[57] Hsu CH, Lin SY. Rapid examination of the kinetic process of intramolecular lactamization of gabapentin using DSC-FTIR. Thermochim Acta 2009;486(1–2):5–10.
[58] Prankerd RJ. Aspartame. Anal Profiles Drug Subst 2002;29:7–55.